HHS Public Access

Author manuscript

Genesis. Author manuscript; available in PMC 2025 February 01.

Published in final edited form as:

Genesis. 2024 February ; 62(1): e23584. doi:10.1002/dvg.23584.

Generation of a Dcx-CreER^{T2} knock-in mouse for genetic manipulation of newborn neurons

Gabriella A. Perez[1], **Kyung-Won Park**[1], **Denise Lanza**[2], **Jenna Cicardo**[1], **M. Danish Uddin**[1], **Joanna L. Jankowsky**[1,3]

[1]Department of Neuroscience, Baylor College of Medicine, Houston, TX 77030

[2]Department of Molecular and Human Genetics, Baylor College of Medicine, Houston, TX 77030

[3]Departments of Neurology, Neurosurgery, and Molecular and Cellular Biology, Huffington Center on Aging, Baylor College of Medicine, Houston, TX 77030

Abstract

A wide variety of CreER^{T2} driver lines are available for genetic manipulation of adult-born neurons in the mouse brain. These tools have been instrumental in studying fate potential, migration, circuit integration, and morphology of the stem cells supporting lifelong neurogenesis. Despite a wealth of tools, genetic manipulation of adult-born neurons for circuit and behavioral studies has been limited by poor specificity of many driver lines targeting early progenitor cells and by the inaccessibility of lines selective for later stages of neuronal maturation. We sought to address these limitations by creating a new CreER^{T2} driver line targeted to the endogenous mouse doublecortin locus as a marker of fate-specified neuroblasts and immature neurons. Our new model places a T2A-CreER^{T2} cassette immediately downstream of the Dcx coding sequence on the X chromosome, allowing expression of both Dcx and CreER^{T2} proteins in the endogenous spatiotemporal pattern for this gene. We demonstrate that the new mouse line drives expression of a Cre-dependent reporter throughout the brain in neonatal mice and in known neurogenic niches of adult animals. The line has been deposited with the Jackson Laboratory and should provide an accessible tool for studies targeting fate-restricted neuronal precursors.

Keywords

Adult neurogenesis; hippocampus; dentate gyrus; subgranular zone; olfactory bulb; neural progenitor; doublecortin; CreER

Correspondence: Joanna L. Jankowsky, Department of Neuroscience, Baylor College of Medicine, One Baylor Plaza, Mail Stop BCM295, Houston, TX 77030; phone: 713 798 8337; fax: 713 798 3946; jankowsk@bcm.edu.

Author contributions: GAP, JC, and MDU performed mouse experiments, husbandry, and imaging; KWP and DL constructed the CRISPR targeting vector and generated the mouse line; JLJ conceived the study, obtained funding, and wrote the manuscript with input from GAP.

Conflict of interest: The authors have no financial or non-financial competing interests to declare.

Ethics statement: All animal work presented here was reviewed and approved by the Baylor College of Medicine Institutional Animal Care and Use Committee.

Introduction

Studies of adult hippocampal neurogenesis have become increasingly refined over the last 60 years, advancing from early work with radioactive DNA analogues to current experiments involving targeted genetic manipulations (Imayoshi, Sakamoto, & Kageyama, 2011; Owji & Shoja, 2020). Fate mapping has given way to molecular analysis using transgenic tools to precisely control neural progenitors and their progeny. Maturation of adult born neurons has been meticulously delineated into distinct developmental stages characterized by specific molecular markers (Kempermann, Jessberger, Steiner, & Kronenberg, 2004; Kempermann, Song, & Gage, 2015). The field has curated an extensive toolkit for genetically accessing these cells, using CreER^{T2} drivers to induce recombination at precise stages of neurogenesis (Imayoshi et al., 2011).

Despite their utility, genetic driver lines are not without limitation. Two primary challenges in the genetic manipulation of neurogenesis are specificity and accessibility. Ectopic recombination beyond the intended neurogenic population can occur either through inadvertent CreER^{T2} (CreER) expression in non-native patterns or through endogenous expression in cell types sharing a common protein marker. Either situation can confound attribution of behaviors governed by the targeted neural population. The former has been reported in several transgenic nestin-CreER lines where partial promoter elements and random chromosomal insertion site collaborate to produce ectopic CreER expression (Imayoshi et al., 2011; Sun, Yetman, Lee, Chen, & Jankowsky, 2014). The latter scenario arises when using CreER driver lines based on stem cell markers like GLAST and GFAP that are shared by a wide array of non-neurogenic astrocytes (Imayoshi et al., 2011). Even accurately targeted neural stem cells will introduce genetic alterations in multiple non-neuronal cell types, as all progeny inherit the modification. One way to address these concerns would be to express CreER using promoters associated with more restricted markers of neuronal fate, such as doublecortin (Dcx). Within the adult brain, Dcx emerges in fate-restricted, dividing type 2b neuroblasts, marking these cells for 2–3 weeks as they differentiate into immature neurons (Kempermann et al., 2004; Kempermann et al., 2015; Terreros-Roncal et al., 2023). Employing the Dcx promoter to drive CreER expression might prevent recombination in non-neuronal cell types derived from multi-potent stem cells. Furthermore, targeting the recombinase to the endogenous Dcx locus would reduce the risk of ectopic expression that can result from transgenic approaches.

In addition to the biological considerations surrounding specificity, the accessibility of many neurogenic driver lines poses another challenge. Of the numerous nestin-CreER lines published by 2012, only two are readily available from public repositories (Jackson Laboratory #16261, (Lagace et al., 2007); Riken RBC #RBRC05998 (Imayoshi, Ohtsuka, Metzger, Chambon, & Kageyama, 2006)). A similar constraint extends to driver lines designed for more restricted neural progenitors using the Dcx promoter, with none of the four published lines readily accessible (Cheng et al., 2011; Jablonska et al., 2010; Werner et al., 2012; Zhang et al., 2010) (N.B., one unpublished transgenic Dcx-CreER line has been deposited at MMRRC, #32780-MU). We sought to overcome these biological and technical limitations by creating a new CreER mouse line targeting the Dcx locus and making this line available through Jackson Laboratory as a shared resource for the

neurogenesis community. Our strategy allows expression of both Dcx and CreER with spatial and temporal specificity, resulting in widespread recombinase activity in the neonatal brain that contracts to neurogenic niches in the subgranular (SGZ) and subventricular zones (SVZ) of the adult.

Results and Discussion

We incorporated the tamoxifen-inducible CreER^{T2} cassette into the 3' end of the mouse doublecortin (Dcx) locus immediately following the terminal amino acid M366 within exon 7. The sequences were separated by a T2A peptide to generate two independent proteins. This design ensured retention of endogenous Dcx function while introducing tamoxifen-dependent Cre recombinase (Figure 1A, B). Two founder lines with accurate targeting were established and subsequently bred with the Ai3 Cre reporter line to produce bigenic offspring in which we could test the efficiency and specificity of tamoxifen (tam)-induced recombination (Madisen et al., 2010). Neonatal mice from each cross received 2–3 tam injections between postnatal day 4 and 12, and were euthanized 2–10 days after the final injection. Brain tissue from these mice revealed robust and widespread neuronal labeling in one line (3443, Figure 1C), but only sparse expression in the other (3440, Figure 1D). As a result, all future experiments used line 3443.

We next tested the effect of tam administration in adult bigenic CreER/Ai3, focusing on the subgranular zone (SGZ) and subventricular zone (SVZ) where neurogenesis continues throughout adulthood. Through a series of experiments, we administered tam for 3 consecutive days to mice ranging from 6 to 61 weeks of age, and euthanized animals between 11 and 76 days post injection (dpi).

In young adult mice (6–10 wk of age) that were euthanized ~2 wk after the final injection, we saw strong labeling in the olfactory bulb (OB) and variable labeling in the SGZ (Figure 2A). Cells labeled with yellow fluorescent protein (YFP) had the morphology of neurons in both regions. Of the four previous Dcx-CreER lines where reporter labeling is described, our knock-in line exhibited stronger labeling in OB but comparatively weaker labeling in the rostral migratory stream [(Jablonska et al., 2010; Werner et al., 2012; Zhang et al., 2010) but see (Cheng et al., 2011)]. However, accurate comparison is complicated by variations in tam dosages, treatment durations, and post-injection time intervals.

In addition to the SGZ and OB, we also saw scattered neuronal labeling throughout the cortex and striatum. Infrequent labeling was also noted in hippocampal pyramidal and subicular neurons, cerebellar Purkinje neurons, and the septal area. Several of these regions express endogenous Dcx at low levels (Gomez-Climent et al., 2008; La Rosa et al., 2020; Nacher, Crespo, & McEwen, 2001), and other Dcx-CreER transgenic lines have reported similar labeling outside of canonical neurogenic zones (Cheng et al., 2011; Werner et al., 2012; Zhang et al., 2010). A significant portion of the ectopic labeling seen after tam injection was also apparent in CreER;Ai3 mice without tam treatment (Figure 2B). In contrast, no labeling was seen in Ai3 mice lacking CreER. These findings suggest that the ectopic labeling observed in non-neurogenic regions of untreated CreER;Ai3 mice, along

with a proportion of on-target OB labeling, was due to tam-independent recombination (Figure 2C).

The pattern of YFP labeling in our new Dcx-CreER mice was strikingly different than we have found with nestin-CreER lines using the same Ai3 reporter allele (Sun et al., 2014). While labeling of SGZ was similar in the Dcx- and nestin-CreER lines we tested, they diverged considerably in the degree of SVZ labeling. The nestin mice displayed robust SVZ labeling in all three lines we examined (Figures 3A and B and data not shown), whereas the Dcx-CreER mice exhibited little if any labeling in this region (Figure 3C). Dcx and nestin models also differed in the extent of ectopic labeling. Dcx mice showed relatively few YFP+ cells beyond the main neurogenic zones, in contrast to the widespread labeling observed in two of three tested nestin-CreER lines (Dranovsky et al., 2011; Imayoshi et al., 2006). These particular lines showed unexpectedly dense YFP expression in cerebellum, with one line additionally labeling pyramidal neurons in deep cortical layers and CA1, while the other labeled a scattered mix of astrocytes and neurons throughout the brain. Among the nestin-CreER lines we tested, only one showed the expected specificity for SGZ and SVZ (Lagace et al., 2007). However, we note that the expression differences highlighted here may vary with treatment conditions. We also note that our comparison is not entirely accurate as tam dosing, duration, and interval before harvest differed between our prior work on the nestin lines and our current work on the Dcx model. Nevertheless, our findings suggest that the Dcx model may provide improved specificity for adult-born neurons, attributable to two key factors: 1) targeting a later marker of neuronal maturation, and 2) modifying the endogenous locus rather than using a transgenic promoter fragment.

The efficiency of tam-induced YFP expression in Dcx-CreER;Ai3 mice was consistently strong within the OB for the small number of mice where we examined this region (n=4, data not shown). Tam-induced labeling within the SGZ was more variable between animals (Figure 4). This assessment is based on 11 mice between 8–10 wk of age, injected with tam for 3 consecutive days, and harvested 11–16 days post injection (dpi). However, this group was somewhat variable, with both male (n=3) and female animals (n=8), on C57BL/6 (B6; n=4) and FVBB6 backgrounds (n=7), sectioned coronally or horizontally. A small number of animals (n=4) was examined after a second round of 3 tam injections administered 1 wk after completion of the initial 3 injections. This modified dosing regimen yielded more robust and consistent labeling within the SGZ (data not shown). This observation suggests that the tam dose and frequency can be optimized to improve recombination efficiency in SGZ. Because our approach incorporated CreER into the endogenous Dcx locus, our model expressed only a single copy of the recombinase. This feature may necessitate extended tam administration to achieve maximal activation, in contrast to transgenic models that express higher levels of CreER under control of artificial promoters.

Dcx is typically expressed in fate-restricted type 2b neuroblasts, marking these cells for 2–3 weeks as they differentiate into immature neurons (Kempermann et al., 2004; Terreros-Roncal et al., 2023). Consistent with this timing, YFP+ cells in Dcx-CreER;Ai3 animals harvested 12 d post-tam had the appearance of immature neurons. These cells exhibited dendrites extending into the middle and outer molecular layers of the dentate gyrus, accompanied by initial signs of axonal projections into CA3 (Figure 5A, C). By 2.5 mo

after tam injection, labeled cells had progressed into mature granule neurons, evidenced by complex dendritic trees and dense axonal signal in the hilus and CA3 (Figure 5B, D). In the coronal sections used for this experiment, YFP labeling could also be seen in the piriform cortex and was prominent in animals harvested at late times after tam injection (Figure 5C–D). Dcx+ neurons in this region have been reported in mammalian species from rodents to primates (Fasemore et al., 2018; Luzzati, Bonfanti, Fasolo, & Peretto, 2009; Nacher et al., 2001; Pekcec, Loscher, & Potschka, 2006; Shapiro et al., 2007; van Groen et al., 2021), and have been fate-mapped using a prior Dcx-CreER line to generate a novel type of cortical complex cell (Benedetti et al., 2020). Co-immunofluorescence for YFP and native Dcx revealed minimal overlap between the two markers in animals harvested 11–16 days after tam (Figure 5E). This observation suggests that our model may capture neuroblasts as they are exiting the Dcx+ stage. By 23 d post-tam, many YFP+ cells co-labeled for NeuN, confirming they had indeed matured into granule neurons (Figure 5F).

In our final experiment, we compared the extent of labeling in young and old Dcx-CreER;Ai3 animals. Bigenic animals were treated with tam either at 8–10 wk (n=7) or 56–61 wk of age (n=3). Both groups were harvested 15 d after the final injection. Notably, labeling within the SGZ declined sharply in the aged animals, while labeling in the OB remained strong by comparison (Figure 6). Neurogenesis is reported to decline similarly with age in both regions (Apple, Solano-Fonseca, & Kokovay, 2017), suggesting that the higher brightness of the OB relative to other brain regions likely masked a quantitative decline in cell numbers.

The new Dcx-CreER knock-in model presents several advantages over transgenic Dcx-CreER strains, notably its availability through the Jackson Laboratory. The new line also allows for labeling of immature neurons in both OB and SGZ, setting it apart from previously published Dcx-CreER models which primarily label SGZ (Cheng et al., 2011) or SVZ (Jablonska et al., 2010). Dcx-CreER lines may also prove valuable in targeting fate-committed neuroblasts and immature neurons, as opposed to multipotent stem and amplifying progenitor cells targeted by nestin-CreER models (Imayoshi et al., 2011). However, these advantages do come with potential drawbacks. Foremost, Dcx is located on the X chromosome, which complicates breeding compared to other CreER models where the transgene is autosomal. Our Dcx-CreER knock-in model must be bred through the female if CreER-positive male offspring are needed. In addition, the potential for X inactivation in female Dcx-CreER mice might result in mosaic recombination. Although we have not investigated the impact of sex on recombinase efficiency, this factor should be considered when working with this model. Ultimately, the advantage of temporal precision in defining the labeled population will need to be weighed against the challenge associated with an X-linked insertion to determine when and where this model will best serve.

Methods.

Building the DCX-T2A-CreER^{T2} DNA template.

We designed a DNA template that would introduce a T2A-CreER^{T2} cassette in-frame immediately following the Dcx terminal amino acid M366 within exon 7. The T2A-CreER^{T2} targeting construct was built in several steps.

First, we created a 5' Dcx arm to add the T2A sequence in place of the stop codon. The Dcx 5' arm was amplified from mouse genomic DNA using forward primer GCGCGCCGCGGGTATCCGATAATCTCATGTTGTAA and reverse primer TTCCTCTGCCCTCCATGGAATCGCCAAGTGAATCA. The second fragment containing T2A and a short piece of the Dcx 5' arm was amplified from pAAV-TRE3G-GlyCl-YFP-GlyCl (Sun et al., 2014) using forward primer GGCGATTCCATGGAGGGCAGAGGAAGTCTGC and reverse primer GCGCGGCGGCCGCTGGGCCAGGATTCTCCTCGA. These two fragments were combined by Gibson assembly using forward primer GCGCGCCGCGGGTATCCGATAATCTCATGTTGTAA and reverse primer GCGCGGCGGCCGCTGGGCCAGGATTCTCCTCGA. The resulting fragment containing the Dcx 5' arm plus the complete T2A sequence was digested with SacII and NotI, and ligated into cloning vector L4440 (Addgene #1654) cut with the same enzymes to generate L4440-Dcx5'. Subsequently, CreER^{T2} was amplified from pCreER^{T2} (Feil, Wagner, Metzger, & Chambon, 1997) using forward primer GCGCGGCGGCCGCAATGTCCAATTTACTGACCGTACA and reverse primer GCGCGGCTAGCTCAAGCTGTGGCAGGGAAACC. The resulting CreER^{T2} fragment was digested with NotI and NheI, and ligated to L4440-Dcx5' cut with the same enzymes to generate L4440-Dcx5'-CreER^{T2}. Finally, the DCX 3' arm was amplified from mouse genomic DNA using forward primer GCGCGGCTAGCAAGATGATAAGCTAAATCAAAGCC and reverse primer GCGCGCCCGGGGGAGCCTGAAGAGTTTTGCTC. The resulting Dcx 3' fragment was digested with NheI and SmaI and ligated to L4440-Dcx5'-CreER^{T2} cut with the same enzymes to generate the final homology-guided fragment containing a portion of Dcx intron 6 and exon 7 upstream of the stop codon, a fragment of exon 7 and intron 7 downstream of the stop codon, and the inserted T2a-CreER^{T2} sequence.

sgRNA and Cas9 mRNA preparation.

A DNA template for guide RNA transcription was generated by PCR from overlapping DNA oligonucleotides (Bassett, Tibbit, Ponting, & Liu, 2013). After purification, a single guide RNA (sgRNA; 5' GATTCCATGTGAAAGATGAT (AGG); WGE ID 565727900) was synthesized by in vitro transcription using the MEGAshortscript T7 kit (ThermoFisher, AM1354) and purified using the MEGAclear Transcription Clean-Up Kit (ThermoFisher AM1908). All samples were analyzed by Nanodrop to determine concentration and visualized by Qiaxcel Advanced System to check for RNA quality using the RNA QC V2.0 kit. Cas9 mRNA was transcribed using the mMESSAGE mMACHINE T7 Ultra Transcription Kit (ThermoFisher, AM1345) from linearized plasmid DNA pX330 (Addgene, 42230) modified to include a T7 promoter.

Generation of the long single-stranded DNA repair donor for CRISPR/Cas9-mediated genome editing.

The Dcx-T2A-CreER^{T2} plasmid was used as a template for amplification using 5' phosphorylated forward primer 5' ACCTTTTAGGGGAAGCTGAGT and reverse primer 5' GGCCCAGAAGAGAAGTCACA. The primers were chosen to produce homology arms of 160–250 nucleotides in length, and 12 PCR reactions of 50 ul each were run using Q5

high fidelity polymerase (NEB, M0491) to generate sufficient yield for subsequent steps. The resulting 2466 bp PCR product was purified using the QIAquick PCR Clean-up Kit (Qiagen, 28104), then digested using lambda exonuclease (NEB, M0262) according to the manufacturer's protocol, and purified once more using the Monarch PCR & DNA Cleanup Kit (NEB, T1030).

Embryo injection.

190 pronuclear stage C57BL/6J embryos were microinjected as described previously (Lanza et al., 2018) with 50 ng/ul Cas9 mRNA, 10 ng/μl guide RNA, and 50 ng/μl long single-stranded Dcx-T2A-CreER^{T2} DNA; 151 embryos were transferred into 5 ICR pseudopregnant females, resulting in 2 correctly targeted offspring from 6 live pups.

DCX-CreER^{T2} founder verification to establish the line.

The two correctly targeted offspring from CRISPR/Cas9 embryos were bred to C57BL/6J mates to test germline transmission. Both founders transmitted the CreER^{T2} transgene and their transgenic offspring were then outcrossed to Ai3 reporter mice on a mixed strain background (available from The Jackson Laboratory on a pure C57BL/6J background as B6.Cg-*Gt(ROSA)26Sor*$^{tm3(CAG-EYFP)Hze}$/J, stock # 007903) (Madisen et al., 2010). Of the two founders, Line 3443 provided higher recombination efficiency upon tamoxifen treatment was selected for further study. CreER^{T2}-positive offspring from the Ai3 outcross were selected for the absence of the reporter allele, and heterozygous CreER^{T2} animals were backcrossed to C57BL/6J (stock #000664) for an additional 7 generations once the Ai3 allele was removed. Genotyping was performed by PCR using Cre forward primer GCC GAA ATT GCC AGA ATC AG and reverse primer ACA TTG GTC CAG CCA CCA GC along with MAPT positive control forward primer CTC AGC ATC CCA CCT GTA AC and reverse primer CCA GTT GTG TAT GTC CAC CC. Transgenic animals produce a 430 bp band, all animals should exhibit a 187 bp control band. These mice have been deposited with The Jackson Laboratory as stock #038595, C57BL/6J-*Dcx*$^{em1(cre/ERT2)Jjan}$/J.

Nestin-CreER mice.

Nestin-CreER^{T2} mice referred to here as Line H on a hybrid B6129 background were kindly provided by Rene Hen (Dranovsky et al., 2011); nestin-CreER^{T2} Line 4 mice on a congenic C57BL/6 background were kindly provided by Ryoichiro Kageyama (Imayoshi et al., 2006). Prior analysis of these lines is described in Sun et al. (Sun et al., 2014).

Tamoxifen administration.

Tamoxifen (Sigma T5648) was dissolved by sonication in a mix of 200 proof molecular biology grade ethanol (Fisher, BP2818-500) and sunflower seed oil (Sigma S5007) at a ratio of 1:9 ethanol:oil based on a protocol from Amelia Eisch. Once dissolved, tamoxifen solution was stored in the dark at 4°C for up to 1 wk. Juvenile animals were injected s.c. with 180 mg/kg tamoxifen solution for 2 or 3 d between postnatal day 4 and 12. Adult animals were injected i.p. with 180 mg/kg tamoxifen solution daily for 3 to 5 d. In some cases, we tested a repeated dosing regimen of 2 × 3 d with a week recovery between rounds.

Tissue harvest and immunofluorescence.

Tamoxifen treated adult mice were harvested by transcardial perfusion with PBS followed by 4% paraformaldehyde in PBS. Adult animals were harvested between 2–23 d after the final dose of tamoxifen (most at 15 dpi), or in one case after 76 d following final dose. Juvenile mice were euthanized without perfusion. Brains were extracted and postfixed by immersion in 4% paraformaldehyde at 4° C for 3 hr or overnight. Brain tissue was equilibrated in PBS containing 30% sucrose and then frozen on dry ice. Tissue sections were cut at 35 um using a freezing sliding microtome, and stored in cryoprotectant until immunostaining.

DCX and GFP:

Immunostaining was performed as described previously (Zhao et al., 2022). Briefly, sections were rinsed three times with PBS to remove cryoprotectant and then blocked for 1 hr at RT in PBS containing 0.5% Triton X-100 and 10% normal goat serum. Sections were then incubated overnight at 4° C in block containing chicken anti-GFP antibody (1:1,000, Abcam ab13970) and rabbit anti-doublecortin (1:200, Cell Signaling Technology 4604S). After three washes with PBS, sections were incubated for 2 hr at RT in block containing goat anti-chicken Alexa 488 antibody (Life Technologies A11039) and goat anti-rabbit 568 antibody (Life Technologies A11036) each diluted 1:500. Sections were washed with PBS before being mounted onto SuperFrost Plus slides (Fisher Scientific 12-550-15) using Prolong Diamond Antifade Mounting Medium (Molecular Probes/Fisher P36970).

NeuN and GFP:

Immunostaining was performed as described above except sections were rinsed with TBS before blocking for 1 hr at RT with TBS containing 0.3% Triton X-100 and 5% normal goat serum. Sections were then incubated overnight at 4° C with chicken anti-GFP antibody (1:1,000, Abcam, ab13970) and rabbit anti-NeuN (1:500, Abcam 177487). After washing with TBS, sections were incubated for 2 hr at RT in block containing goat anti-chicken Alexa 488 antibody (Life Technologies A11039) and goat anti-rabbit 568 antibody (Life Technologies A11036) each diluted 1:500. Sections were washed with TBS before being mounted as above.

Acknowledgements:

We thank Caleb Wood for expert assistance with microscopic imaging, the BCM Genetically Engineered Rodent Model Core for assistance making the Dcx-CreER mouse model, and Melissa Comstock and Jennifer Saldana for support with mouse husbandry.

Funding:

This work was supported by R01 NS092615, RF1 AG058188, RF1 AG054160, and HHMI GT13620 to JLJ. The Genetically Engineered Rodent Model Core at BCM is funded in part by the National Institutes of Health Cancer Center Grant (P30 CA125123).

Data availability:

The data supporting this study are contained within the manuscript itself. The Dcx-CreERT2 model described here will be available from The Jackson Laboratory as stock #038595, C57BL/6J-*Dcx*$^{em1(cre/ERT2)Jjan}$/J.

Abbreviations:

B6	C57BL/6J
Dcx	doublecortin
dpi	days post injection (measured from the final day)
GLAST	glial glutamate and aspartate transporter (EAAT1; Slc1a3)
GFAP	glial fibrillary acidic protein
OB	olfactory bulb
SGZ	subgranular zone
SVZ	subventricular zone
tam	tamoxifen
YFP	yellow fluorescent protein

References

Apple DM, Solano-Fonseca R, & Kokovay E (2017). Neurogenesis in the aging brain. Biochem Pharmacol, 141, 77–85. doi:10.1016/j.bcp.2017.06.116 [PubMed: 28625813]

Bassett AR, Tibbit C, Ponting CP, & Liu JL (2013). Highly efficient targeted mutagenesis of Drosophila with the CRISPR/Cas9 system. Cell Rep, 4(1), 220–228. doi:10.1016/j.celrep.2013.06.020 [PubMed: 23827738]

Benedetti B, Dannehl D, Konig R, Coviello S, Kreutzer C, Zaunmair P, . . . Couillard-Despres S. (2020). Functional Integration of Neuronal Precursors in the Adult Murine Piriform Cortex. Cereb Cortex, 30(3), 1499–1515. doi:10.1093/cercor/bhz181 [PubMed: 31647533]

Cheng X, Li Y, Huang Y, Feng X, Feng G, & Xiong ZQ (2011). Pulse labeling and long-term tracing of newborn neurons in the adult subgranular zone. Cell Res, 21(2), 338–349. doi:10.1038/cr.2010.141 [PubMed: 20938464]

Dranovsky A, Picchini AM, Moadel T, Sisti AC, Yamada A, Kimura S, . . . Hen. (2011). Experience dictates stem cell fate in the adult hippocampus. Neuron, 70(5), 908–923. doi:10.1016/j.neuron.2011.05.022 [PubMed: 21658584]

Fasemore TM, Patzke N, Kaswera-Kyamakya C, Gilissen E, Manger PR, & Ihunwo AO (2018). The Distribution of Ki-67 and Doublecortin-Immunopositive Cells in the Brains of Three Strepsirrhine Primates: Galago demidoff, Perodicticus potto, and Lemur catta. Neuroscience, 372, 46–57. doi:10.1016/j.neuroscience.2017.12.037 [PubMed: 29289719]

Feil R, Wagner J, Metzger D, & Chambon P (1997). Regulation of Cre recombinase activity by mutated estrogen receptor ligand-binding domains. Biochem Biophys Res Commun, 237(3), 752–757. doi:10.1006/bbrc.1997.7124 [PubMed: 9299439]

Gomez-Climent MA, Castillo-Gomez E, Varea E, Guirado R, Blasco-Ibanez JM, Crespo C, . . . Nacher J. (2008). A population of prenatally generated cells in the rat paleocortex maintains an immature

neuronal phenotype into adulthood. Cereb Cortex, 18(10), 2229–2240. doi:10.1093/cercor/bhm255 [PubMed: 18245040]

Imayoshi I, Ohtsuka T, Metzger D, Chambon P, & Kageyama R (2006). Temporal regulation of Cre recombinase activity in neural stem cells. Genesis, 44(5), 233–238. doi:10.1002/dvg.20212 [PubMed: 16652364]

Imayoshi I, Sakamoto M, & Kageyama R (2011). Genetic methods to identify and manipulate newly born neurons in the adult brain. Front Neurosci, 5, 64. doi:10.3389/fnins.2011.00064 [PubMed: 21562606]

Jablonska B, Aguirre A, Raymond M, Szabo G, Kitabatake Y, Sailor KA, . . . Gallo V. (2010). Chordin-induced lineage plasticity of adult SVZ neuroblasts after demyelination. Nat Neurosci, 13(5), 541–550. doi:10.1038/nn.2536 [PubMed: 20418875]

Kempermann G, Jessberger S, Steiner B, & Kronenberg G (2004). Milestones of neuronal development in the adult hippocampus. Trends Neurosci, 27(8), 447–452. [PubMed: 15271491]

Kempermann G, Song H, & Gage FH (2015). Neurogenesis in the Adult Hippocampus. Cold Spring Harb Perspect Biol, 7(9), a018812. doi:10.1101/cshperspect.a018812 [PubMed: 26330519]

La Rosa C, Cavallo F, Pecora A, Chincarini M, Ala U, Faulkes CG, . . . Bonfanti L. (2020). Phylogenetic variation in cortical layer II immature neuron reservoir of mammals. Elife, 9. doi:10.7554/eLife.55456

Lagace DC, Whitman MC, Noonan MA, Ables JL, DeCarolis NA, Arguello AA, . . . Eisch AJ. (2007). Dynamic contribution of nestin-expressing stem cells to adult neurogenesis. J Neurosci, 27(46), 12623–12629. doi:27/46/12623 [pii]10.1523/JNEUROSCI.3812-07.2007 [PubMed: 18003841]

Lanza DG, Gaspero A, Lorenzo I, Liao L, Zheng P, Wang Y, . . . Heaney JD. (2018). Comparative analysis of single-stranded DNA donors to generate conditional null mouse alleles. BMC Biol, 16(1), 69. doi:10.1186/s12915-018-0529-0 [PubMed: 29925370]

Luzzati F, Bonfanti L, Fasolo A, & Peretto P (2009). DCX and PSA-NCAM expression identifies a population of neurons preferentially distributed in associative areas of different pallial derivatives and vertebrate species. Cereb Cortex, 19(5), 1028–1041. doi:10.1093/cercor/bhn145 [PubMed: 18832334]

Madisen L, Zwingman TA, Sunkin SM, Oh SW, Zariwala HA, Gu H, . . . Zeng H. (2010). A robust and high-throughput Cre reporting and characterization system for the whole mouse brain. Nat Neurosci, 13(1), 133–140. doi:10.1038/nn.2467 [PubMed: 20023653]

Nacher J, Crespo C, & McEwen BS (2001). Doublecortin expression in the adult rat telencephalon. Eur J Neurosci, 14(4), 629–644. doi:10.1046/j.0953-816x.2001.01683.x [PubMed: 11556888]

Owji S, & Shoja MM (2020). The History of Discovery of Adult Neurogenesis. Clin Anat, 33(1), 41–55. doi:10.1002/ca.23447 [PubMed: 31381190]

Pekcec A, Loscher W, & Potschka H (2006). Neurogenesis in the adult rat piriform cortex. Neuroreport, 17(6), 571–574. doi:10.1097/00001756-200604240-00003 [PubMed: 16603913]

Shapiro LA, Ng KL, Kinyamu R, Whitaker-Azmitia P, Geisert EE, Blurton-Jones M, . . . Ribak CE. (2007). Origin, migration and fate of newly generated neurons in the adult rodent piriform cortex. Brain Struct Funct, 212(2), 133–148. doi:10.1007/s00429-007-0151-3 [PubMed: 17764016]

Sun MY, Yetman MJ, Lee TC, Chen Y, & Jankowsky JL (2014). Specificity and efficiency of reporter expression in adult neural progenitors vary substantially among nestin-CreER(T2) lines. J Comp Neurol, 522(5), 1191–1208. doi:10.1002/cne.23497 [PubMed: 24519019]

Terreros-Roncal J, Flor-Garcia M, Moreno-Jimenez EP, Rodriguez-Moreno CB, Marquez-Valadez B, Gallardo-Caballero M, . . . Llorens-Martin M. (2023). Methods to study adult hippocampal neurogenesis in humans and across the phylogeny. Hippocampus, 33(4), 271–306. doi:10.1002/hipo.23474 [PubMed: 36259116]

van Groen T, Kadish I, Popovic N, Caballero Bleda M, Bano-Otalora B, Rol MA, . . . Popovic M. (2021). Widespread Doublecortin Expression in the Cerebral Cortex of the Octodon degus. Front Neuroanat, 15, 656882. doi:10.3389/fnana.2021.656882 [PubMed: 33994960]

Werner L, Muller-Fielitz H, Ritzal M, Werner T, Rossner M, & Schwaninger M (2012). Involvement of doublecortin-expressing cells in the arcuate nucleus in body weight regulation. Endocrinology, 153(6), 2655–2664. doi:10.1210/en.2011-1760 [PubMed: 22492306]

Zhang J, Giesert F, Kloos K, Vogt Weisenhorn DM, Aigner L, Wurst W, & Couillard-Despres S (2010). A powerful transgenic tool for fate mapping and functional analysis of newly generated neurons. BMC Neurosci, 11, 158. doi:10.1186/1471-2202-11-158 [PubMed: 21194452]

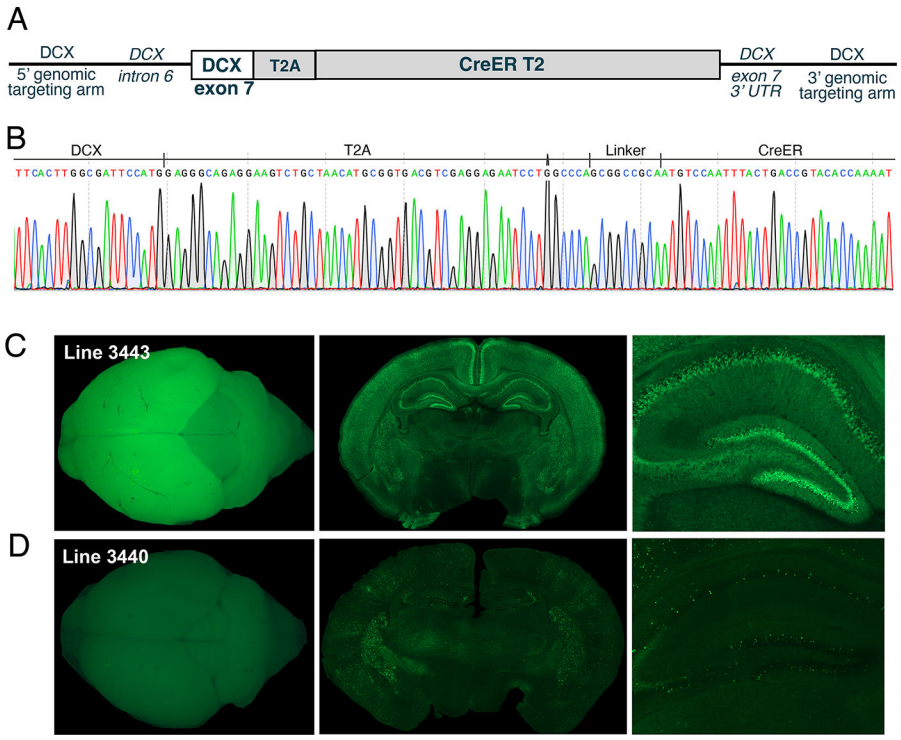

Figure 1. Allele design and validation of tamoxifen response in neonatal brain.

A. The targeting construct replaced the stop codon in exon 7 to insert an in-frame T2A-CreER^{T2} cassette immediately downstream of the Dcx coding sequence.

B. Sanger sequencing across the insertion site confirmed the position and reading frame of the T2A-CreER^{T2} cassette. The portion of sequence shown here covers the last 5 amino acids of the endogenous Dcx gene, the complete T2A sequence, a 3-alanine residue linker, and the first 10 amino acids of CreER^{T2}.

C-D. CRISPR/Cas9 targeting of B6 embryos produced two Dcx-CreER founder animals that were each bred to the Ai3 Cre reporter line. Bigenic CreER;Ai3 offspring were injected with tam 2–3 times between postnatal day 4 and 12 (180 mg/kg, s.c.) and were euthanized between postnatal day 14 and 21. The left panels show intact fixed brains, the middle panels show coronal brain sections, and the right panels show the dorsal hippocampus. All panels show native fluorescence from female offspring. Line 3443 produced strong YFP fluorescence throughout the brain following tam administration (**B**). Line 3440 produced sparse YFP expression and was culled (**C**). Exposure was increased and gamma decreased to allow visualization of sparse YFP labeling in tissue from Line 3440.

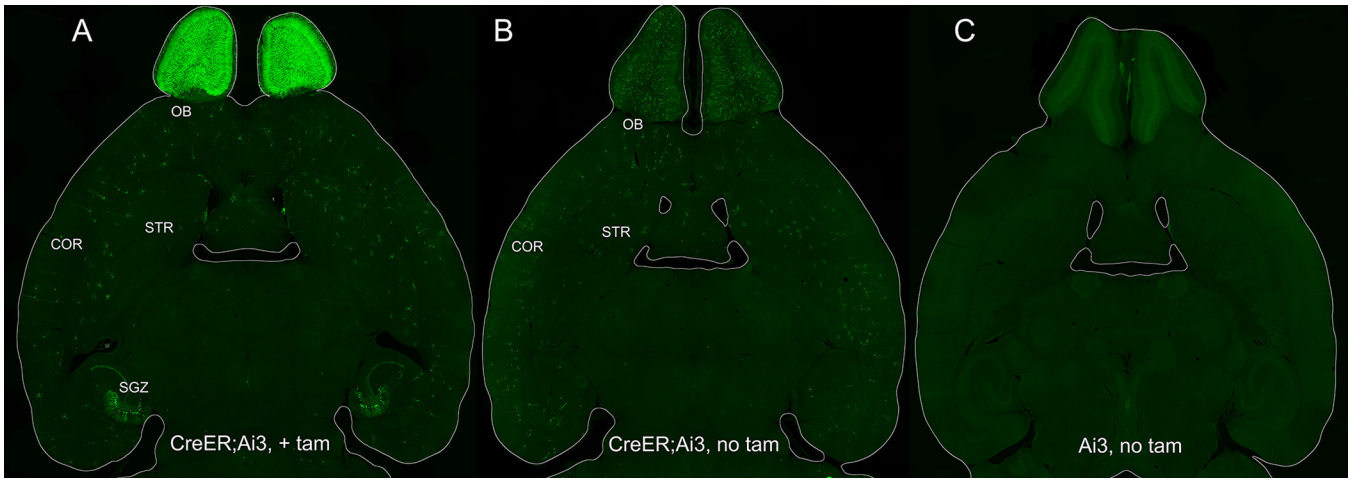

Figure 2. Tamoxifen-dependent recombination and tamoxifen-independent leak.

A. Representative Dcx-CreER;Ai3 mouse injected with tam (3 d x 180 mg/kg, i.p.) at 9 wk of age and harvested 15 dpi. COR, cortex; STR, striatum

B. Untreated Dcx-CreER;Ai3 mouse harvested at 9 wk of age showed the extent of tam-independent recombinase activity.

C. Ai3 single transgenic animal showed no YFP expression in the brain, therefore YFP+ cells in untreated bigenic mice resulted from leaky Cre activity and not Cre-independent reporter expression. All images show YFP-immunostained tissue from female animals on a B6 background.

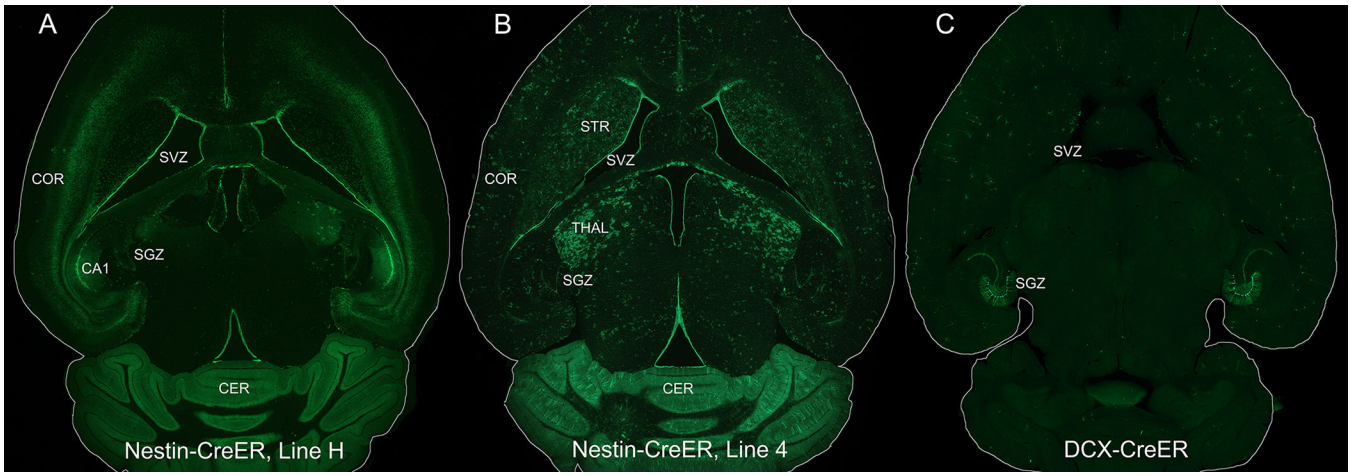

Figure 3. Comparison of reporter labeling in nestin-CreER lines with Dcx-CreER.

A. Bigenic offspring of nestin-CreER mice from the Hen lab (Line 'H') crossed with the Ai3 Cre reporter line. Mice were injected with tam (5 d x 180 mg/kg, i.p.) at 8 wk of age and harvested 7 d after final injection. COR, cortex, CER, cerebellum

B. Bigenic offspring of Line 4 nestin-CreER mice from the Kageyama lab crossed with Ai3 and treated with tam as in panel A. Both nestin-CreER lines H and 4 showed strong reporter expression in the SVZ and SGZ (the latter is less apparent here), but also displayed ectopic labeling in cerebellum, cortex, and multiple other brain areas.

C. Dcx-CreER;Ai3 bigenic animals were treated with tam (3 d x 180 mg/kg) at 9 wk of age and harvested 15 d after final injection. YFP+ cells were found in SGZ and OB (not shown), but absent from the SVZ at this time point, with scattered labeling in cortex and striatum, however, ectopic activity was considerably lower than either nestin-CreER line.

All tissue was immunostained for YFP; all mice were on a B6 background. Nestin-CreER panels reproduced with permission from Sun et al. (Sun et al., 2014)

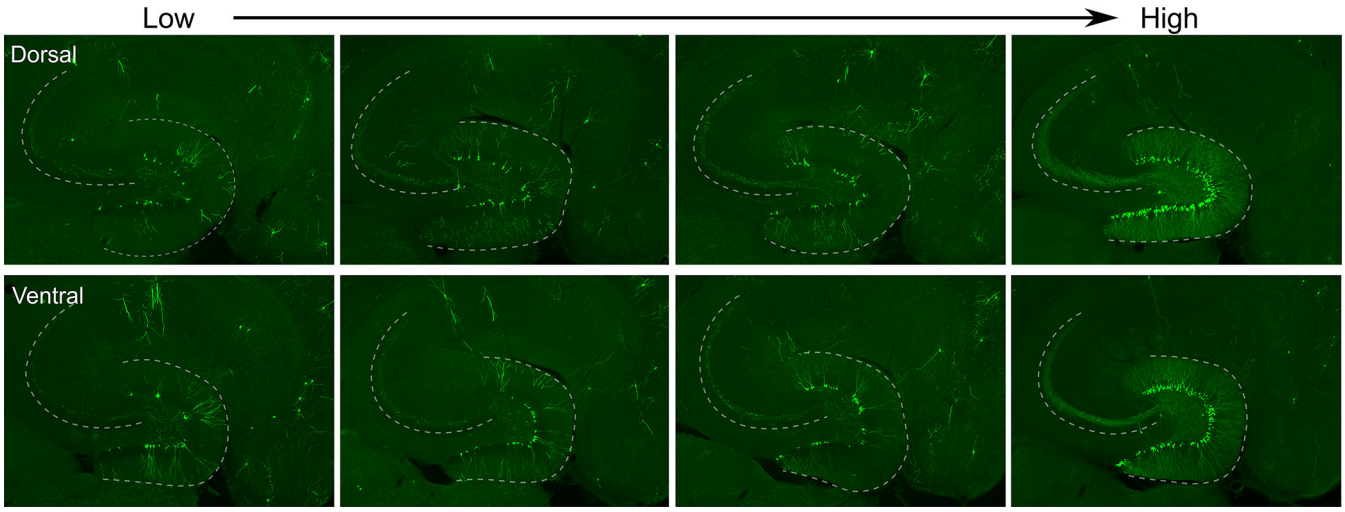

Figure 4. Dcx-CreER displays variable SGZ labeling across animals.

Dcx-CreER;Ai3 bigenic female mice on a FVBB6 background were injected with tam (3 d x 180 mg/kg, i.p.) at 8–9 wk of age and harvested 15 dpi. Four representative animals are shown here. Horizontal sections were immunostained for YFP; images were taken from dorsal and ventral planes for each animal. The density of YFP-labeled cells varied widely between mice, despite matched treatment conditions. Variance may decrease with longer tam treatment (i.e., 5 d x 180 mg/kg, or dual rounds of 3 d x 180 mg/kg) data not shown).

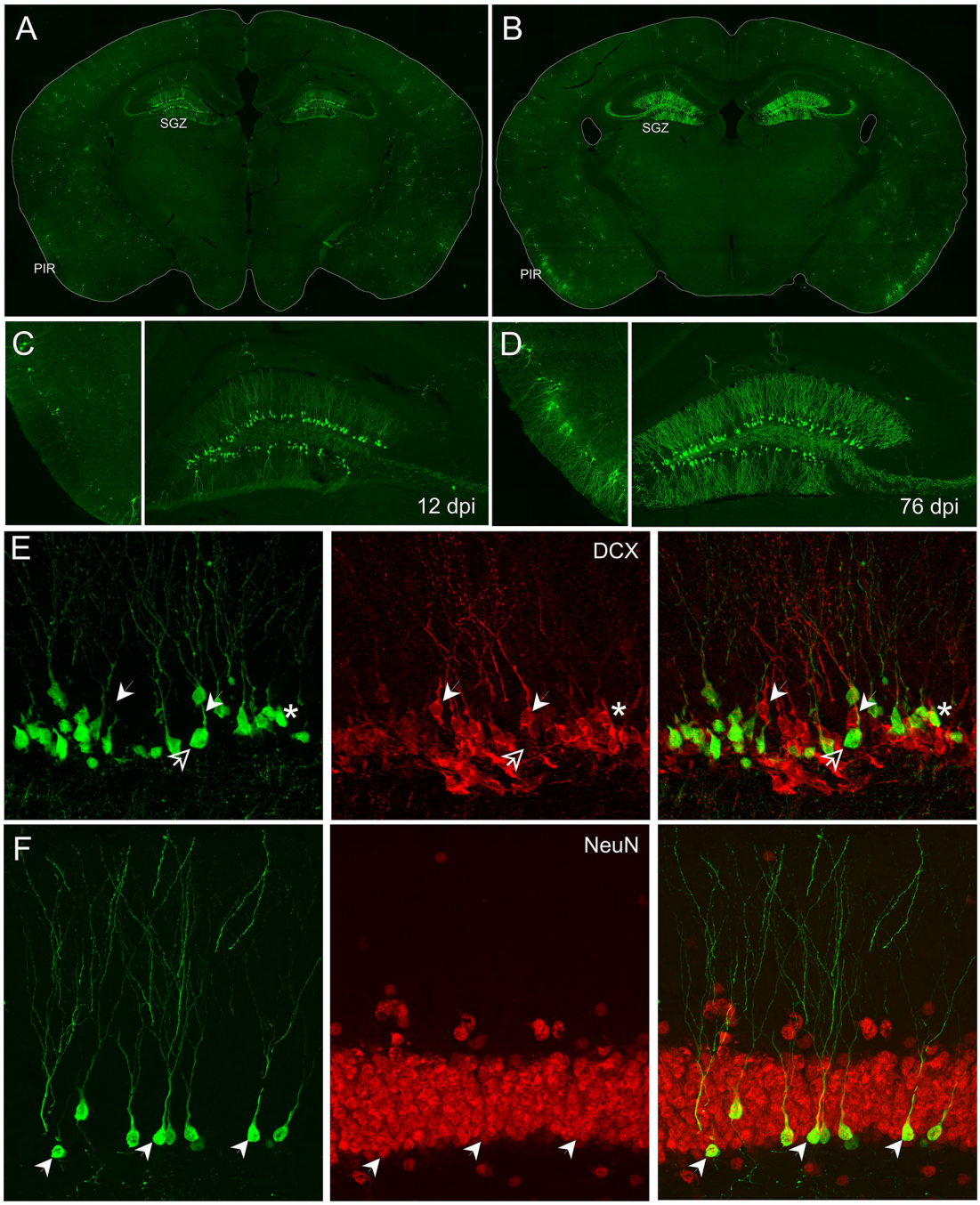

Figure 5. Labeled SGZ cells mature into neurons.

A-B. Neurites continue to elaborate with time post-tam. Dcx-CreER;Ai3 females on a B6 background were injected with tam (2–3 d x 180 mg/kg, i.p.) at 8–10 wk of age and harvested 12 (A) or 76 dpi (B). PIR, piriform cortex.

C-D. High magnification insets taken from panels A and B showing YFP+ cells in the piriform cortex (left) and SGZ (right).

E. Co-immunostaining for YFP (*green*) and Dcx (*red*) revealed that only rare YFP+ cells are still Dcx+ (*asterisk*) at 12 dpi. At this time point, many YFP cells lack Dcx (*open arrow*),

while most Dcx+ cells are not labeled with YFP (*arrowhead*). The animal shown was a B6 bigenic female injected with tam 3d x 180 mg/kg at 10 wk and harvested 12 dpi.
F. Co-immunostaining for YFP (*green*) and NeuN (*red*) reveals that most YFP+ cells have become NeuN+ (*arrowhead*) by 23 dpi. The animal shown was a FVBB6 bigenic male injected with tam 3d x 180 mg/kg twice with a 1 wk interval, harvested 23 dpi.

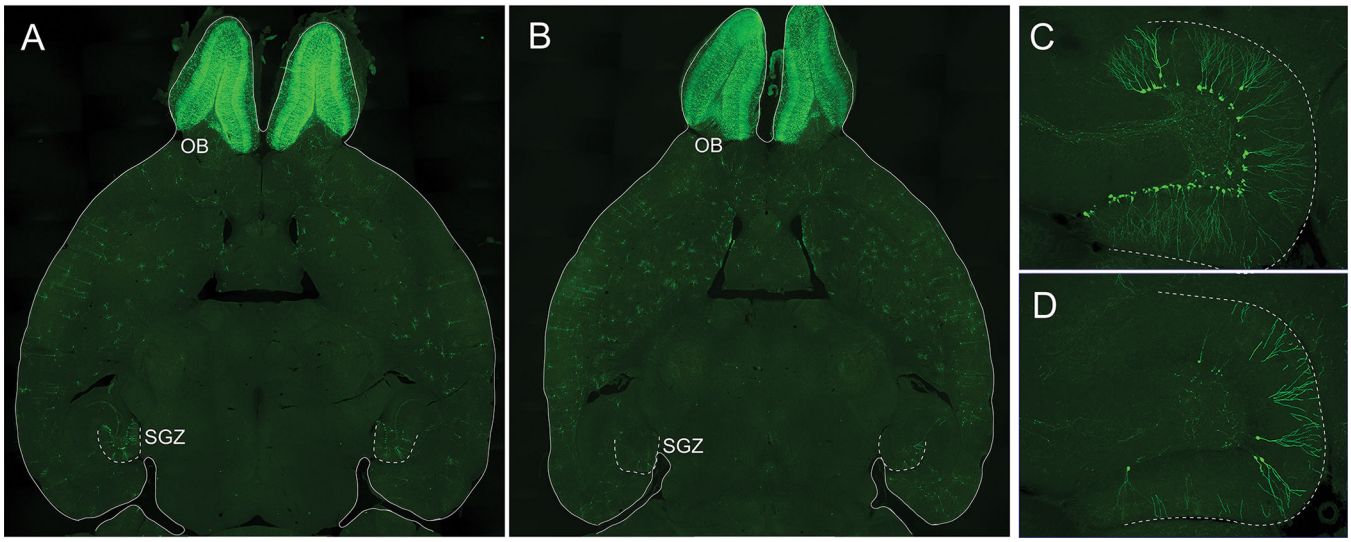

Figure 6. Labeling in SGZ decreases to a greater extent with age than OB.

A-B. Bigenic Dcx-CreER;Ai3 mice on a B6 background injected with tam (3 d x 180 mg/kg, i.p.) at 10 wk of age (A) or 61 wk (B) and harvested 14–15 dpi. Although labeling in the OB remains prominent, closer examination shows a decline in the density of labeled OB cells in the aged animals; the drop in YFP labeling with age is more apparent in the SGZ. Ectopic labeling in the cortex and striatum was unaffected by age.

C-D. YFP labeling in the dentate gyrus of bigenic Dcx-CreER;Ai3 mice on a FVBB6 background injected with tam (3 d x 180 mg/kg, i.p.) at 6 wk of age (C) or 52 wk (D) and harvested 14–15 dpi.

Young animals shown here were female, aged mice were male.